RP Materials: Proceedings
Vol. 3, Part 1 (2023) pp. 22–27
e-ISSN: 2583-8342

RESEARCH PLATEAU PUBLISHERS

Cite this article: I. Maity, S. Biswas, Structural and electronic properties of 2D transition metal dichalcogenides: MoS_2 and $MoSe_2$, *RP Materials: Proceedings* Vol. 3, Part 2 (2024) pp. 22–27.

Original Research Article

Structural and electronic properties of 2D transition metal dichalcogenides: MoS_2 and $MoSe_2$

Indranil Maity[1,*], Saurabhi Biswas[2]

[1]Department of Electronics and Communication Engineering (ECE), Institute of Engineering and Management (IEM), University of Engineering and Management (UEM), Kolkata, West Bengal, India

[2]Department of Electronics and Communication Engineering (ECE), Institute of Engineering and Management (IEM), Kolkata, West Bengal, India

[*]Corresponding author, E-mail: indrasanu026@gmail.com

[**]Selection and Peer-Review under responsibility of the Scientific Committee of the International Conference on Composite Materials for Environment Protection & Remediation 2024 (ICCMEPR 2024).

ARTICLE HISTORY
Received: 2 July 2024
Revised: 12 August 2024
Accepted: 14 August 2024
Published online: 19 August 2024

KEYWORDS
TMDs; MoS_2; $MoSe_2$; Bond length; HOMO-LUMO; ESP; DOS.

ABSTRACT

The 2D-Transition Metal Dichalcogenides (TMDs) are an arena of huge interest as potential materials for gas sensor applications due to their unique properties. The present report is based on the structural and electronic properties of two most commonly studied TMDs for gas sensing, molybdenum disulfide (MoS_2), and molybdenum diselenide ($MoSe_2$). The studies were carried out using the Density Functional Theory (DFT) as implemented in the Gaussian 09W and Gauss View 6.0 suits. The structural properties reported includes the 2×2 lattice optimised structure of MoS_2 and $MoSe_2$ along with their calculated corresponding bond lengths. The Mo-S bond length was found to be 2.42 Å and Mo-Se as 2.60 Å, which is almost equal to the experimental values. One crucial electronic parameter reported is the highest occupied molecular orbital (HOMO), and lowest unoccupied molecular orbital (LUMO) with their corresponding energy values, which further gives the HOMO-LUMO gap, which in turn is a very important parameter that greatly influences the performance of gas sensors. The HOMO-LUMO gap was found to be 0.024 eV in case of MoS_2 and 0.029 eV for $MoSe_2$. The Electrostatic Potential (ESP) plot gives an overview of the reactive sites present in the molecule for electrophilic or nucleophilic attacks. The DOS spectrum obtained using the Gauss Sum software provides an idea about the number of available states at a particular energy level of the molecule. The study of the structural and electronic properties of MoS_2 and $MoSe_2$ is essential for understanding and further optimising their performance as sensing materials.

1. Introduction

Two-dimensional (2D) materials have garnered substantial interest from researchers across various disciplines, including physics, chemistry, and material science due to their unique properties. These materials find numerous applications in the arena of gas sensing, catalysis and great storage devices [1]. A significant category of 2D materials are the transition metal dichalcogenides (TMDs). The main features which make these materials potential sensing materials are their high carrier mobility, large surface area, quick response to changes in environments and higher concentration of reactive sites which leads to high activity [2-3]. Molybdenum Disulphide (MoS_2) a significant member of the family of TMDs has recently gathered significant interest due to its intrinsic bandgap, high electron mobility, outstanding electrical properties, quick recovery and good chemical stability as compared to other materials [4, 1-2].

Understanding the structural properties: crystal structure, orientation, bond length; and electronic properties: HOMO-LUMO, Density of States (DOS) and Electrostatic Potential (ESP) of MoS_2 (molybdenum disulphide) and $MoSe_2$ (Molybdenum Diselenide) is crucial for their gas sensing applications because these properties directly influence how gas molecules interact with the material [5]. These combined structural and electronic characteristics dictate the sensor's overall performance, including response and recovery times, making a thorough understanding of these properties vital for optimizing gas sensing technologies [6-7].

This paper presents a detailed report on the structural and electronic properties of pristine MoS_2 and $MoSe_2$. A geometrically optimized structure was obtained using DFT calculations, and various properties such as the HOMO-LUMO, ESP, DOS and bond length were investigated. To the best of our knowledge, there have been no reports on the detailed electro-chemical properties of pristine MoS_2 and $MoSe_2$ at one place.

2. Computational details

The pristine MoS_2 and $MoSe_2$ sheet that was taken for study, shown in Figure1 and Figure 5, consisted of a 2X2 lattice crystal with 4 molybdenum (Mo) atoms, and 8 (S), and (Se) atoms, respectively. First principle DFT calculations were used to carry out the experiment to find the properties of MoS_2

Copyright: © 2024 by the authors. Licensee Research Plateau Publishers, India
This article is an open access article distributed under the terms and conditions of the Creative Commons Attribution (CC BY) license (https://creativecommons.org/licenses/by/4.0/).

and $MoSe_2$ sheet based on their structure and electronic configurations using the Gaussian 09W and Gauss View 6.0 suits. The optimized structures were obtained by using the Density Functional Theory, B3LYP (Becke, 3-parameter, Lee-Yang-Parr) functional with 3-21G as the basis set. B3LYP functional combines the local density approximation (LDA) with the gradient-corrected correlation functional [8]. The bond length, HOMO-LUMO and ESP plots were obtained using the above-mentioned software. The DOS graph was obtained for all the combinations using the Gauss Sum software with the molecular data obtained after optimisation of the molecule.

The HOMO-LUMO gap of the MoS_2 and $MoSe_2$ was calculated from the following equation:

$$E_{HOMO\text{-}LUMO\ gap} = E_{LUMO} - E_{HOMO} \qquad (1)$$

where, E_{HOMO} stands for the highest occupied orbital molecular energy, E_{LUMO} means the lowest unoccupied orbital molecular energy of the molecule after optimization and $E_{HOMO\text{-}LUMO\ gap}$ stands for the HOMO-LUMO gap of the molecule which is a very vital parameter for judging the performance of any sensors.

3. Results and discussion

3.1 Structural properties of molybdenum disulphide

The structure of MoS_2 is a hexagonal prism with Mo atom at the centre, covalently bonded with six S atoms, whereas there exists weak van der Waals forces between the sandwiched layers. This is the reason why MoS_2 can be peeled into layers easily, which makes single or few layer MoS_2 synthesis possible [9-10].

The bond length of MoS_2 is a pivotal factor for estimating the structural integrity and properties of the material according to various applications. The bond length observed from the optimised structure of MoS_2 from Figure 1 is 2.42 Å, which signifies a strong covalent bonding between the molybdenum and sulphur atoms within the layer. In monolayer MoS_2, the Mo-S bond length influences the material's band structure and electronic transitions, which in turn impacts its suitability for optoelectronic devices such as photodetectors and transistors. From reported data, it is found that MoS_2has an indirect bandgap of 1.2 eV, and single layer MoS_2 has a direct bandgap of 1.8 eV [11].

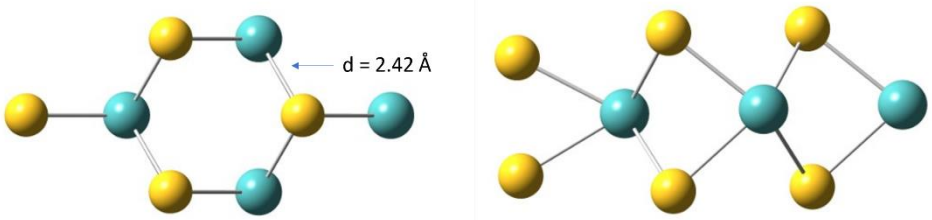

a) Top View b) Side View

Figure 1: Optimized structure of molybdenum disulphide.

3.2 Electronic properties of pristine molybdenum disulphide (MoS_2)

(a) HOMO-LUMO Analysis: The conductivity of MoS_2 is a function of the changes in orbital energy levels [4]. The orbital plots of various levels were generated using GaussView 6.0 software to predict nature of charge transfer between the sensing layer and any other gas/bio molecule [12-13]. The HOMO-LUMO gap is a very important parameter to consider: a smaller gap indicates higher chemical reactivity and lower stability, while a larger gap suggests weaker chemical reactivity and greater stability [14-15].

Varying color gradients of HOMO-LUMO plots as shown in Figure 2 provide insights into the distribution and intensity of these orbitals. Brighter colors, such as red and blue, indicate regions with a high electron density, while colors like green or yellow signify areas with a lower electron density.

The HOMO-LUMO gap another important parameter gives us information about the sensing abilities of the sensor [4]. The orbital energy magnitudes of various orbitals, and the HOMO-LUMO gaps are presented in Table 1. For MoS_2, the HOMO-LUMO gap is found to be +0.02439 eV. This positive value arises because the energy value of the highest orbital is more negative than that of the lowest orbital. A small HOMO-LUMO gap is preferable for gas sensors, as it indicates that a lower amount of energy is required for electrons to go to a higher energy state from a lower one.

Table 1: Orbital energy and HOMO-LUMO band gap calculation of Molybdenum Disulphide (MoS_2).

Molecular orbitals of MoS_2 (Iso value – 0.02)	
E_{HOMO} (eV)	-0.19159
E_{LUMO} (eV)	-0.16720
$E_{HOMO\text{-}1}$ (eV)	-0.21335
E_{LUMO+1} (eV)	-0.15520
$E_{HOMO\ -\ LUMO}$ gap (eV)	0.02439
$E_{HOMO\text{-}1\ -\ LUMO+1}$ gap (eV)	0.05815

(b) ESP Analysis: The Electrostatic Potential (ESP) basically functions as a tool to identify the reactive sites in a molecule, focussing on the regions suitable for electrophilic attacks (red and yellow) and nucleophilic attacks (blue) [16-18]. The ESP for all combinations was generated using GaussView software with an iso value set to 0.004. The ESP colour scheme follows a particular colour code where; red signifies surfaces rich in electrons having partial negative charge, blue represents areas deficient in electrons with partial positive charge, yellow is for slightly electron- rich areas, cyan indicates slightly electron deficient areas and green indicates regions neutral in nature [4, 19-20].

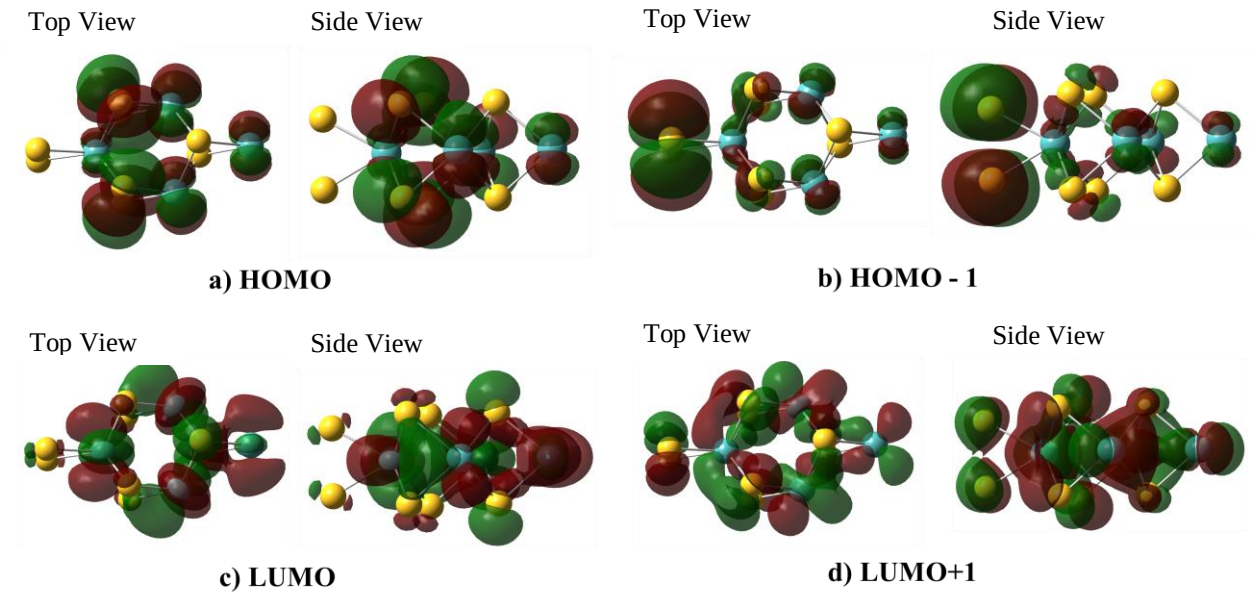

Figure 2: Visual representation of molecular orbitals of molybdenum disulfide (a) HOMO; (b) LUMO; (c) HOMO-1; (d) LUMO+1.

Figure 3 shows the ESP plot of Molybdenum Disulphide with a 3D view, showcasing the different reactive centres within the molecule. The ESP plots were calibrated with potential values ranging from $-5.160e^{-2}$ to $-0.122e^{0}$eV, where each colour follows the colour code mentioned above. A prominently negative electrostatic potential surrounding the interaction site is depicted in orange, covering nearly a large portion of the MoS_2 sheet. Each atom's unique charge distribution and chosen isovalue collectively shape the ESP plot visualization.

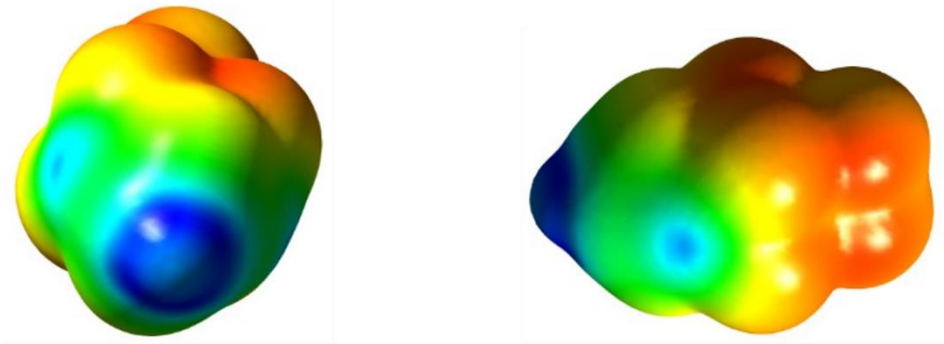

a) Top View b) Side View

Figure 3: Electrostatic potential of pristine molybdenum disulphide.

(c) DOS Analysis: The physical and chemical interactions between sensing layer and gas/bio molecule, along with their electronic properties is investigated using the density of states analysis. The results of the DOS spectrum of MoS_2 monolayer is depicted in Figure 8. The gap near the Fermi level signifies the semiconductor characteristics of the MoS_2 layer [1]. DOS presents an overview of the levels of electronic energy within the conduction and valance bands [2]. The green lines in a DOS spectrum represent the HOMO levels, whereas the red lines correspond to the LUMO levels of MoS_2 [18].

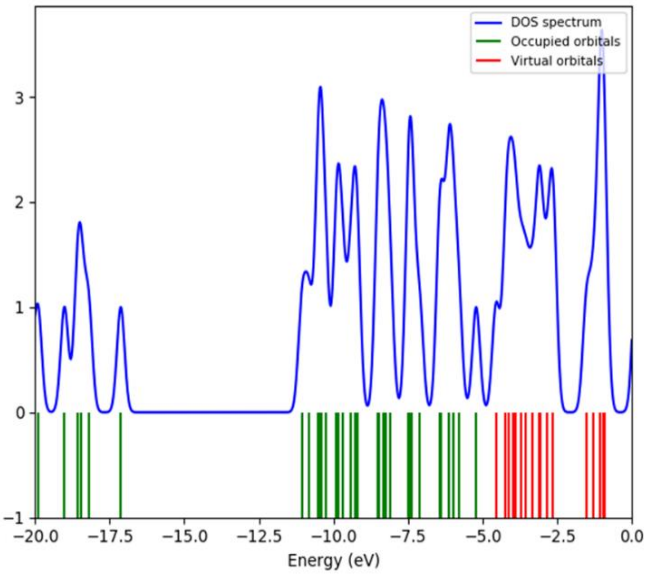

Figure 4: Density of states of pristine molybdenum disulphide.

3.3 Structural properties of molybdenum diselenide ($MoSe_2$)

The structure of $MoSe_2$ is similar to that of MoS_2, made of strongly bonded Se-Mo-Se covalent bonds and weak van der Waals forces between the sandwiched layers [21]. Similarly $MoSe_2$ can also be made into sheets confirming its high crystal quality. The bond length observed from the optimised structure of $MoSe_2$ is 2.60 Å, which signifies a strong covalent bonding between the molybdenum and selenium atoms, but a less strong interaction in comparison with MoS_2.

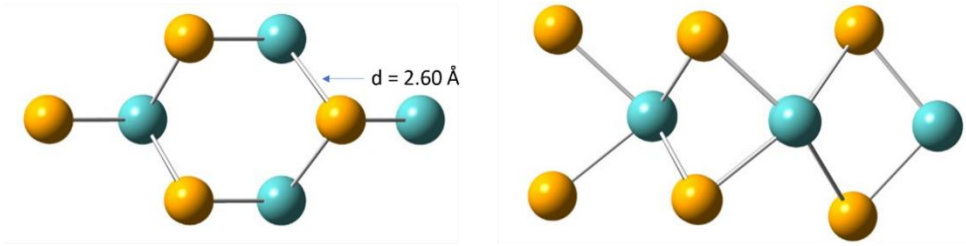

a) Top View b) Side View

Figure 5: Optimized structure of molybdenum diselenide.

3.4 Electronic properties of pristine molybdenum diselenide

(a) HOMO-LUMO Analysis: As stated before conductivity of a material is a function of the changes in HOMO-LUMO energies. The orbital energy magnitudes of various orbitals, and the HOMO-LUMO gaps are presented in Table 2. For $MoSe_2$, the HOMO-LUMO gap is approximately 0.02876 eV, greater than that of MoS_2. Due to the larger HOMO-LUMO gap, we can infer that $MoSe_2$ has higher kinetic stability and low chemical reactivity as compared to MoS_2.

(b) ESP Analysis: The ESP was generated using the GaussView software in a similar manner. The iso value was set to 0.004. Figure 7 shows the ESP plot of Molybdenum Diselenide with a 3D view, showcasing the different reactive centres within the molecule. The ESP plots were calibrated with potential values from $-7.960e^{-3}$ to $4.000e^{-2}$eV, where each colour follows the colour code mentioned above. We can see, as compared to MoS_2 the red areas are greater in case of $MoSe_2$, proving that $MoSe_2$ is more nucleophilic in nature than MoS_2.

Table 2: Orbital energy and HOMO-LUMO band gap calculation of Molybdenum Diselenide ($MoSe_2$).

Molecular orbitals of $MoSe_2$ (Iso value – 0.02)	
E_{HOMO} (eV)	-0.18214
E_{LUMO} (eV)	-0.15338
E_{HOMO-1} (eV)	-0.19378
E_{LUMO+1} (eV)	-0.13563
$E_{HOMO-LUMO}$ gap (eV)	0.02876
$E_{HOMO-1-LUMO+1}$ gap (eV)	0.01775

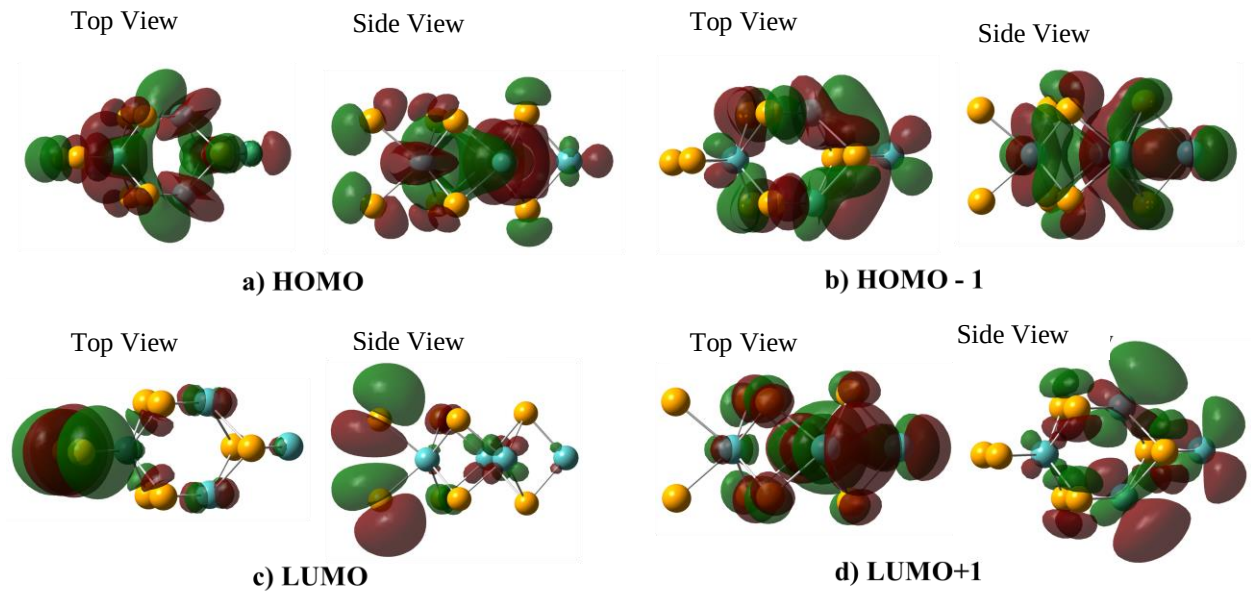

Figure 6: Visual representation of molecular orbitals of molybdenum diselenide (a) HOMO; (b) LUMO; (c) HOMO-1; (d) LUMO+1.

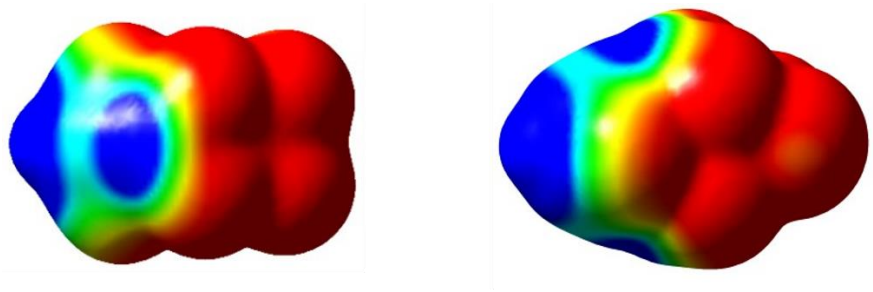

a) Top View b) Side View

Figure 7: Electrostatic potential of pristine molybdenum diselenide.

(c) DOS Analysis: The DOS spectrum was obtained in the same manner as that of MoS_2 using the GaussSum software. The meaning of the parameters of a DOS spectrum are already stated. As, we can see the DOS peaks are higher in case of $MoSe_2$ as compared to that of MoS_2. DOS gives an overview of the available states that can be occupied at a specific level. A higher peak of DOS means many states are available for occupation. Especially it becomes an irreplaceable parameter when interaction between surfaces is considered, which involves transition of electrons.

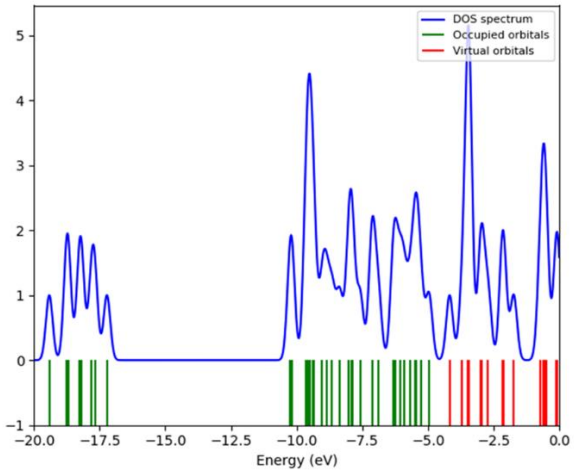

Figure 8: Density of States of Pristine Molybdenum Diselenide.

4. Conclusions

In conclusion, this study deals with an analysis of the structural ad electronic properties of molybdenum disulphide (MoS_2) and molybdenum diselenide ($MoSe_2$), highlighting their use as potential sensing materials. We obtained optimized 2X2 lattice structures and calculated their bond lengths, which closely resembled experimental data (Mo-S: 2.42 Å, Mo-Se: 2.60 Å). The electronic properties include the HOMO-LUMO gaps of the two molecules (0.024 eV for MoS_2 and 0.029 eV for $MoSe_2$), which translates to $MoSe_2$'s higher kinetic stability and low chemical reactivity as compared to that of MoS_2. The Electrostatic Potential (ESP) plots revealed reactive sites essential for understanding interactions with gas molecules, while the density of states (DOS) spectra provided insights into the available electronic states. Overall, our findings highlighted the importance of such properties for optimising and tuning the materials for enhanced sensing performance and paving a way for future applications in this field.

Acknowledgements

The authors are thankful to the Department of ECE, IEM, Kolkata for their support.

References

[1] D. Chen, J. Tang, X. Zhang, Y. Li, H. Liu, Detecting decompositions of sulfur hexafluoride using MoS_2 monolayer as gas sensor, *IEEE Sens. J.* **19** (2019) 39–46.

[2] A.I. Ayesh, DFT investigation of H_2S and SO_2 adsorption on Zn modified $MoSe_2$, *Superlat. Microst.* **162** (2022) 107098.

[3] W. Ai, L. Kou, X. Hu, Y. Wang, A.V. Krasheninnikov, L. Sun, X. Shen, Enhanced sensitivity of $MoSe_2$ monolayer for gas adsorption induced by electric field, *J. Phys. Cond. Mat.* **31** (2019) 445301.

[4] T.E. Gber, H. Louis, A.E. Owen, B.E. Etinwa, I. Benjamin, F.C. Asogwa, M.M. Orosun, E.A. Eno, Heteroatoms (Si, B, N, and P) doped 2D monolayer MoS_2 for NH_3 gas detection, *RSC Adv.* **12** (2022) 25992–26010.

[5] I. Maity, K. Ghosh, H. Rahaman, P. Bhattacharyya, Tuning of electronic properties of edge oxidized armchair graphene nanoribbon by the variation of oxygen amounts and positions, *J. Mater. Sci. Mater. Electron.* **28** (2017) 9039–9047.

[6] I. Maity, D. Acharyya, K. Huang, P. Chung, M. Ho, P. Bhattacharyya, A comparative study on performance improvement of ZnO nanotubes based alcohol sensor devices by PD and RGO hybridization, *IEEE Trans. Electron Dev.* **65** (2018) 3528–3534.

[7] I. Maity, H. Nagasawa, T. Tsuru, P. Bhattacharyya, Correlation between ammonia selectivity and temperature dependent functional group tuning of GO, *IEEE Trans. Nanotechnol.* **20** (2021) 129–136.

[8] I. Maity, K. Ghosh, H. Rahaman, P. Bhattacharyya, Selectivity tuning of graphene oxide based reliable gas sensor devices by tailoring the oxygen functional groups: A DFT study based approach, *IEEE Trans. Dev. Mater. Reliab.* **17** (2021) 738-745.

[9] X. Li, H. Zhu, Two-dimensional MoS_2: Properties, preparation, and applications, *J. Materiomics* **1** (2015) 33–44.

[10] H. Xu, J. Zhu, Q. Ma, J. Ma, H. Bai, L. Chen, S. Mu, Two-dimensional MoS_2: Structural properties, synthesis methods, and regulation strategies toward oxygen reduction, *Micromachines* **12** (2021) 240.

[11] N. Thomas, S. Mathew, K. Nair, K. O'Dowd, P. Forouzandeh, A. Goswami, G. McGranaghan, S. Pillai, 2D MoS_2: structure, mechanisms, and photocatalytic applications, *Mater. Today Sustain.* **13** (2021) 100073.

[12] F. Akman, A density functional theory study based on monolignols: Molecular structure, HOMO-LUMO analysis, molecular electrostatic potential,*Cell. Chem. Technol.* **53** (2019) 243–250.

[13] D. Rai, H. Joshi, A.D. Kulkarni, S.P. Gejji, R.K. Pathak, Electric field effects on aromatic and aliphatic hydrocarbons: A density-functional study, *J. Phys. Chem. A* 111 (2007) 9111–9121.

[14] M.S.I. Aziz, A.J. Orr-Ewing, Development and application of an optical sensor for ethene in ambient air using near infra-red cavity ring down spectroscopy and sample preconcentration, *J. Environ. Monitor.* **14** (2012) 3094.

[15] I. Maity, P. Bhattacharyya, Room temperature acetone sensing performance of RGO-ZNO nanotubes binary hybrid structure, *Sens. Lett.* **17** (2019) 417–422.

[16] A. Mahmood, T. Akram, E.B. De Lima, Syntheses, spectroscopic investigation and electronic properties of two sulfonamide derivatives: A combined experimental and quantum chemical approach, *J. Mol. Struc.* 1108 (2016) 496–507.

[17] Y. Chen, Y. Gui, X. Chen, Adsorption and gas-sensing properties of C_2H_4, CH_4, H_2, H_2O on metal oxides (CuO, NiO) modified SnS_2 monolayer: A DFT study, *Res. Phys.* **28** (2021) 104680.

[18] I. Rajaei, S.N. Mirsattari, Spectroscopic characteristic (FT-IR, 1 H, 13 C NMR and UV–Vis) and theoretical calculations (MEP, DOS, HOMO-LUMO, PES, NBO analysis and keto–enol tautomerism) of new tetradentate N,N′-bis(4-hydroxysalicylidene)-1,4-phenylenediamine ligand as chelating agent for the synthesis of dinuclear Co(II), Ni(II), Cu(II) and Zn(II) complexes, *J. Mol. Struc.* 1163 (2018) 236–251.

[19] P. Politzer, J.S. Murray, The fundamental nature and role of the electrostatic potential in atoms and molecules, *Theor. Chem. Acc.* **108** (2002) 134–142.

[20] L.Z. Fekri, M. Nikpassan, Synthesis, experimental and DFT studies on the crystal structure, FTIR, 1H NMR and 13C NMR spectra of drivatives of dihydropyridines, *J. Chil. Chem. Soc.* **57** (2012) 1415–1421.

[21] S.L. Banu, V. Veerapandy, P. Vajeeston, Structural stability and electronical properties of $MoSe_2$ polymorphs: DFT, *Mater. Today: Proc.* **64** (2022) 1808–1812.

Publisher's Note: Research Plateau Publishers stays neutral with regard to jurisdictional claims in published maps and institutional affiliations.